

1 Sources of variability in methods for processing, storing, and concentrating 2 SARS-CoV-2 in influent from urban wastewater treatment plants

3
4 Joshua A. Steele^{#%}, Amity G. Zimmer-Faust[%], John F. Griffith, Stephen B. Weisberg

5
6 *Southern California Coastal Water Research Project Authority, Costa Mesa, CA, USA*

7 # corresponding author: joshuas@sccwrp.org

8 % these authors contributed equally to this study

9 10 11 **Abstract**

12
13 The rapid emergence of wastewater based surveillance has led to a wide array of SARS-CoV-2 RNA
14 quantification methodologies being employed. Here we compare methods to store samples, inactivate
15 viruses, capture/concentrate viruses, and extract/measure viral RNA from primary influent into
16 wastewater facilities. We found that heat inactivation of the viruses led to a 1-3 log₁₀ decrease
17 compared to chemical inactivation. Freezing influent prior to concentration caused a 1-4 log₁₀ decrease
18 compared to processing fresh samples, but viral capture by membrane adsorption prior to freezing was
19 robust to freeze-thaw variability. Concentration vs. direct extraction, and PCR platform also affected
20 outcome, but by a smaller amount. The choice of nucleocapsid gene target had nearly no effect. Pepper
21 mild-mottle virus was much less sensitive to these methodological differences than was SARS-CoV-2,
22 which challenges its use as a population-level control among studies using different methods. Better
23 characterizing the variability associated with different methodologies, in particular the impact of
24 methods on sensitivity, will aid decision makers in following the effects of vaccination campaigns, early
25 detection of future outbreaks, and potentially monitoring the appearance of SARS-CoV-2 variants in the
26 population.

27 28 29 **1. Introduction**

30
31 Wastewater based surveillance (WBS) of SARS-CoV-2 RNA is gaining traction because of its many
32 advantages over individual testing, particularly the cost-effectiveness of a relatively unbiased pooled
33 sample and the ability to detect virus shed from infected asymptomatic or pre-symptomatic individuals
34 (Bivins et al. 2020, Hart & Halden 2020, Kitajima et al. 2020, Ahmed et al. 2021). WBS also yields
35 information several days and almost two weeks faster than it takes to collate individual testing and
36 hospitalization records, respectively (Nemudryi et al. 2020). As a result, SARS-CoV-2 RNA is being
37 measured in the sewage influent stream throughout the world (Medema et al. 2020, Ahmed et al.
38 2020a, Gerrity et al. 2021, Graham et al. 2021, Gonzalez et al. 2020), from more than 2000 sites in 50
39 countries (Naughton et al. 2021). The application of WBS to SARS-CoV-2 builds upon the success of WBS
40 for monitoring other viral pathogens, including poliovirus, hepatitis A & E, rotavirus, adenovirus, and
41 norovirus (Katayama et al. 2008, Ashgar et al. 2014, Alleman et al. 2021, McCall et al. 2020).

42
43 The rapid emergence of WBS for SARS-CoV-2, though, has led to a wide array of quantification
44 methodologies being employed (Farkas et al. 2020). With little known about the SARS-CoV-2 virus,
45 laboratories had to make decisions about how to inactivate it in samples prior to processing so as to
46 meet safety guidelines. Decisions about extraction and concentration techniques, and whether to use
47 qPCR vs. ddPCR, were largely made based on existing practices with other pathogens within each

48 laboratory, as there was insufficient lead time to measure the effects of such techniques. Target gene
49 selection was often made on availability of primer sets that were initially in scarce supply. Laboratories
50 also had to determine quickly whether to process samples fresh or hold them frozen while they
51 investigated methodological processing details.

52
53 Several studies have looked at the effects of those decisions, the largest of which included 32
54 laboratories processing two sets of common samples (Pecson et al. 2021). That study found up to 7
55 orders of magnitude difference in SARS-CoV-2 concentrations across laboratories when the same
56 samples were processed using different methods, which was considerably larger than within method
57 variability. However, disentangling confounded method effects from such large studies is challenging.
58 There have been a few controlled experiments looking at specific methodological choices, such as
59 concentration techniques (Ahmed et al. 2020b, Torii et al. 2020, La Rosa et al. 2021, LaTurner et al.
60 2021, Whitney et al. 2021) and processing platform (Feng et al. 2021, Cieselski et al 2021, Ahmed et al.
61 2021). Here we expand upon those efforts by conducting controlled experiments to examine a range of
62 sample processing choices (Fig. 1).

63 64 **2. Materials and Methods**

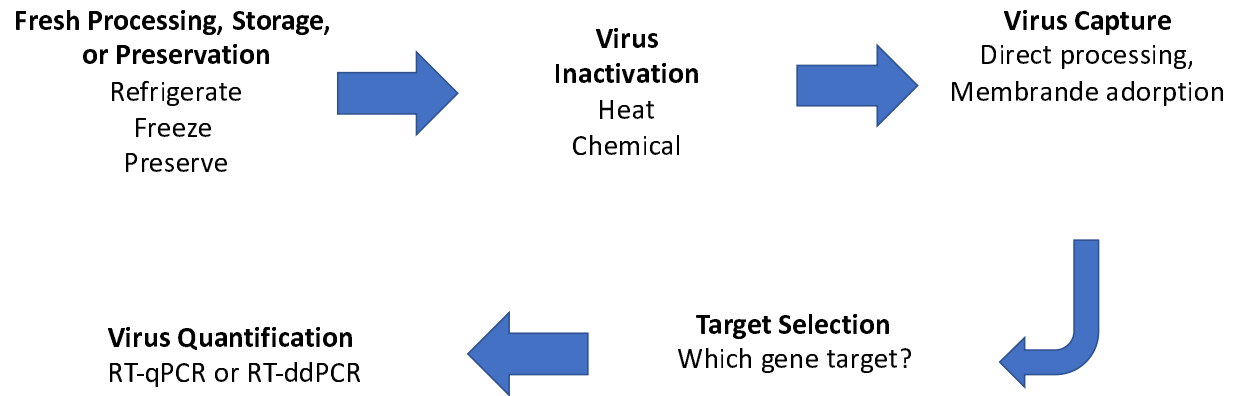
65 66 *2.1 Experimental Design*

67
68 Controlled experiments were performed in two parts (Figure 1). The first set of comparisons tested the
69 effects of freezing and sample storage, heat inactivation, and direct extraction vs concentration on a
70 membrane filter using triplicate influent samples from multiple Southern California WWTPs. For this set
71 of experiments each wastewater sample was aliquoted and processed in parallel three different ways
72 described below (section 2.2). Briefly, 1) the sample was concentrated on a mixed cellulose ester
73 membrane and extracted using bead beating lysis followed by magnetic bead capture; 2) the sample
74 was preserved in lysis buffer and then extracted using bead beating lysis followed by a total nucleic acid
75 magnetic bead capture, and 3) the sample was preserved in DNA/RNA Shield and then extracted using a
76 bead beating lysis followed by silica spin column RNA extraction.

77
78 The second set of comparisons tested the SARS-CoV-2 concentrations measured by two widely used
79 nucleocapsid gene assays (N1: 2019 nCOV N1, N2: 2019 nCOV N2, Table S2) using 296 influent samples
80 from three southern California WWTPs. Thirty of these samples from one WWTP were also used to
81 compare RT-QPCR and RT-droplet digital PCR platform for the SARS-CoV-2 N1 gene. For these
82 comparisons the wastewater sample was concentrated on a mixed cellulose ester membrane then
83 extracted using bead beating lysis followed by magnetic bead capture.

84
85 All comparisons took place on homogenized wastewater samples from five WWTP in Southern
86 California, USA collected and transported to the laboratory at 4°C. Individual WWTP used for each
87 comparison are described in the Supplemental Material (Table S1).

88



89
90

91 Figure 1. Virus in wastewater sample processing steps that were evaluated in this study

92
93

94 *2.1.1 Sample Storage and Preservation*

95

96 Wastewater samples were processed and preserved four different ways. First, samples were
97 immediately processed, extracted, and analyzed via RT-ddPCR on the same day (treatment designation:
98 fresh). Secondly, samples were immediately amended with HCL and MgCl₂ and concentrated on a
99 membrane or amended with lysis buffer (DE:BM) or DNA/RNA shield (DE:Z) and stored at -80°C for at
100 least 24 hours before thawing, extraction and analysis via RT-ddPCR (fresh processed). Third, raw
101 influent was frozen at -80°C for at least one week, then thawed at 4°C and processed following the same
102 protocol as the Fresh samples (frozen). Lastly, raw influent was frozen at -80°C for at least one week and
103 processed following the same protocol as the Fresh Processed samples (frozen X2).

104

105 *2.1.2 Inactivation of Viruses by Heat (Pasteurization)*

106

107 Homogenized wastewater samples were processed two different ways: placed in a water bath at 70°C
108 for 40 minutes or kept at 4°C. For each treatment, a set of samples was concentrated by membrane
109 adsorption and extracted using the bioMerieux magnetic bead extraction kit (HA), or extracted directly
110 from wastewater using the bioMerieux magnetic bead extraction kit (DE:BM) or the Zymo Microbiomics
111 kit (DE:Z).

112

113 *2.1.3 Virus Capture and RNA Extraction*

114

115 Wastewater samples were collected during two different time periods, to evaluate differences between
116 virus capture methods during different levels of background SARS-CoV-2 in the human population.
117 Samples were collected in August 2020, during a period of lower SARS-CoV-2 levels in wastewater, and
118 December 2020, during a period of higher SARS-CoV-2 levels in wastewater.

119

120 *2.1.4 SARS-CoV-2 Gene Target Selection and comparison of gene quantification using RT-QPCR 121 and RT-ddPCR*

122

123 The concentrations of two widely used nucleocapsid gene assays (CDC-N1, CDC-N2) in influent from 296
124 samples across three southern California WWTPs were compared. These samples were processed with
125 the membrane adsorption method (HA) with acidification and MgCl₂ addition (Section 2.7). A subset (n =

126 30) of these samples from one wastewater treatment plant was analysed for SARS-CoV-2 using both RT-
127 QPCR and RT-digital PCR for comparison.

128

129 *2.2 Sample Processing*

130

131 *2.2.1 Virus Adsorption to Mixed Cellulose Ester Filters and Magnetic Bead Extraction (HA)*

132

133 Prior to filtration, bovine coronavirus that was obtained as Bovilis® bovine coronavirus vaccine (Merck &
134 Co Inc, Kenilworth, NJ) was added as a sample processing control for assessing SARS-CoV-2 viral RNA
135 recovery. To collect viruses, wastewater samples were amended to a final concentration of 25
136 mM MgCl₂ and pH of <3.5 through addition of 20% HCl and concentrated on a mixed cellulose
137 ester membrane (type HA: Millipore, Bedford, MA). Samples were filtered in replicate (n=6) for each site
138 and sampling day with 20 mL wastewater concentrated per filter.

139

140 Nucleic acid was extracted the same day using bead beating lysis. HA filters were transferred to pre-
141 loaded 2 mL ZR BashingBead Lysis tubes (Zymo, Irvine, CA, USA) along with the 600 µl NucliSENS lysis
142 buffer. Bead beating was carried out on the Biospec beadbeater (Biospec Products, Bartlesville, OK) for 1
143 minute. After bead beating, total nucleic acids were extracted using the bioMerieux NucliSENS
144 extraction kit and magnetic bead capture (bioMerieux NucliSENS) according to the manufacturer's
145 instructions.

146

147 *2.2.2 Direct Virus Nucleic Acid Extraction via Magnetic Bead Extraction*

148

149 Total nucleic acid was extracted by transferring 750 µl of homogenized raw influent into pre-loaded 2 ml
150 ZR BashingBead Lysis tubes (Zymo Research, Irvine, CA, USA) along with 750 µl NucliSENS lysis buffer
151 and bead beating was carried out on the Biospec beadbeater (Biospec Products, Bartlesville, OK) for 1
152 minute. After bead beating, total nucleic acids were extracted using the bioMerieux NucliSENS
153 extraction kit and magnetic bead capture (bioMerieux NucliSENS) according to the manufacturer's
154 instructions.

155

156 *2.2.3 Direct Virus Nucleic Acid Extraction via Silica Column*

157

158 Total nucleic acid was extracted by transferring 250 µl of homogenized raw influent into pre-loaded 2
159 mL ZR BashingBead Lysis tubes (Zymo Research, Irvine, CA, USA) along with 1.2 ml of DNA/RNA shield
160 (Zymo Research, Irvine, CA). Bead beating was carried out on the Biospec beadbeater (Biospec
161 Products, Bartlesville, OK) for 1 minute. After bead beating, total nucleic acids were extracted using the
162 Zymo Microbiomics RNA Extraction kit (Zymo Research, Irvine, CA) according to the manufacturer's
163 instructions.

164

165 *2.3 Virus Quantification via RT-ddPCR*

166

167 Extracted RNA was analyzed using reverse transcriptase droplet digital PCR (RT-ddPCR) for the N1 and
168 N2 regions of the SARS-CoV-2 N gene, Pepper Mild Mottle Virus (PMMoV), and Bovine Coronavirus
169 (BCoV) genes using the One-Step RT-ddPCR Advanced Kit for Probes (Bio-Rad, Hercules, CA). Primer and
170 probe sequences for SARS-CoV-2 N1 and N2 were those designed by the United States Center for
171 Disease Control (CDC; Lu et al. 2020), PMMoV (Kitajima et al. 2018, Gonzalez et al. 2020), and BCoV
172 (Decaro et al. 2008) are described in table S2. Each primer was added at a final concentration of 0.9 µM
173 and probes were added at a final concentration of .25 µM. 5 µl of RNA extract was added to each

174 reaction for a final volume of 20 μ l. Plates were placed into a Bio-Rad C1000 Touch thermocycler (Bio-
175 Rad, Hercules, CA) and underwent reverse transcription at 50°C for 1 hour. Enzyme activation and initial
176 denaturation were performed at 95°C for 10 minutes, then 40 cycles of denaturation at 95°C for 30
177 seconds, annealing/extension at 58°C for 1 minute. Enzyme deactivation was performed at 98°C for 10
178 minutes followed by a 12°C hold for 20 minutes before being placed in the QX200 (Bio-Rad, Hercules,
179 CA) for droplet reading. For all assays, a minimum of two reactions and a total of $\geq 20,000$ droplets were
180 generated per sample and at least five no template control (NTC) reactions and two positive control
181 reactions were run per 96-well plate as well as extraction-specific NTCs. To consider a sample positive,
182 quantifiable, and included in further analysis, each sample was required to have a minimum of three
183 positive droplets which served as the threshold for the limit of quantification (Cao et al. 2015, Steele et
184 al. 2018). The limit of quantification was converted using the following equation:

$$185 \quad \left(-\ln \left(1 - \frac{\left(\frac{P}{T} \right)}{V_{droplet}} \right) \right) \times \frac{V_{reaction}}{V_{template}}$$

186 Where P is the number of positive droplets, T is the total accepted droplets, $V_{droplet}$ is the average
187 volume per droplet expressed in microliters (i.e. $\sim 0.0009 \mu$ l which is equal to ~ 0.9 nanoliters), $V_{reaction}$ is
188 the volume of the digital PCR reaction, and $V_{template}$ is the volume of sample extract (PCR template)
189 added to the reaction. This per μ l template reaction can then be converted to copies per ml by
190 multiplying by the volume of sample extract divided by the volume of sample filtered (Steele et al.
191 2018). RNA recovery was also assessed using the BCoV exogenous control. Samples where recovery fell
192 below 3% were excluded from further analyses.

193

194 2.4 Virus Quantification via RT-qPCR

195

196 One-step reverse transcription quantitative PCR (RT-qPCR) was used to quantify the N1 and N2 regions
197 of the SARS-CoV-2 N gene. Bio-Rad iTaq Universal Probes One-Step Kit was used according to the
198 manufacturer's instructions (Bio-Rad, Hercules CA). Each primer was added at a final concentration of
199 0.9 μ M and probes were added at a final concentration of 0.25 μ M. 5 μ l of RNA extract was added to
200 each reaction for a final volume of 20 μ l. The IDT 2019-nCoV_N_Positive Control plasmid (IDT, San
201 Diego, CA) was used to make a standard curve. The plasmid was linearized using Xmn1 restriction
202 enzyme in 1X rCutSmart™ Buffer (New England BioLabs, Ipswich, MA) at 37°C for 1 hour followed by
203 denaturation at 65°C for 20 minutes. A 6-point standard curve was created by diluting the linearized
204 plasmid covering a range from 10^6 - 10^1 copies per reaction. Plates were placed into a CFX 96 Touch
205 thermocycler (Bio-Rad, Hercules, CA) and underwent reverse transcription at 50°C for 10 minutes.
206 Enzyme activation and initial denaturation were performed at 95°C for 3 minutes, then 40 cycles of
207 denaturation at 95°C for 15 seconds, annealing/extension at 58°C for 30 seconds. To consider a sample
208 positive and included in further analysis, both reactions The limit of quantification for the wastewater
209 was calculated to be 1000 copies per 100ml sample based on the lowest Cq value obtained on the
210 standard curve: 34.5. The standard curve regression equation was $3.205x+37.26$ ($r^2=0.997$) with an
211 efficiency of 105.1%. All NTCs did not amplify.

212

213 2.5 Data Analysis and Statistics

214

215 Statistical analyses throughout this report were conducted in R (R Core Team 2020), utilizing \log_{10} -
216 transformed concentrations. Analysis of Variance (ANOVA) tests were conducted to assess for significant
217 differences in concentration among the different experimental treatments. Separate ANOVA tests were
218 completed for each target measured (SARS-CoV-2 N2, SARS-CoV-2 N2, PMMoV). When a significant

219 difference was found, the multcomp package in R (Hothorn et al. 2008) was used to run post hoc Tukey
220 comparisons for individual pairwise comparisons between the different treatment levels.

221

222 3. Results

223

224 3.1 Freezing of influent and preserved or concentrated samples

225

226 Freezing Influent samples at -80°C (frozen treatment) and processing through direct extraction resulted
227 in 1-5 log₁₀ lower recoveries compared to fresh influent kept for less than one day at 4°C (fresh
228 treatment), while influent samples processed using membrane adsorption showed little effect of
229 freezing at ultra-low temperatures. Freezing the influent at -80°C resulted in a significant reduction of
230 the SARS-CoV-2 N1 and N2 concentrations by direct extraction for both the Zymo (DE:Z) and the
231 bioMerieux kits (DE:BM) of approximately 2-4 Log₁₀ and more than 4 Log₁₀, respectively, to samples
232 held at 4°C and processed the same day. For the bioMerieux kit, SARS-CoV-2 N1 (F=22.13, all pairwise p-
233 values <0.001) and SARS-CoV-2 N2 (F=91.63, all pairwise p-values<0.001) concentrations were
234 significantly lower for all frozen samples. For the Zymo kit, SARS-CoV-2 N1 (F=4.384, p<0.05) and SARS-
235 CoV-2 N2 (F=4.562, all pairwise p-values <0.05) concentrations were significantly lower for the frozen X2
236 samples only. In contrast, freezing the influent resulted in no significant change in both SARS-CoV-2 N1
237 (F=1.418, all pairwise p-values >0.05) and SARS-CoV-2 N2 concentrations (F=2.009, all pairwise p-values
238 >0.05) for samples concentrated by membrane adsorption (Fig. 2).

239

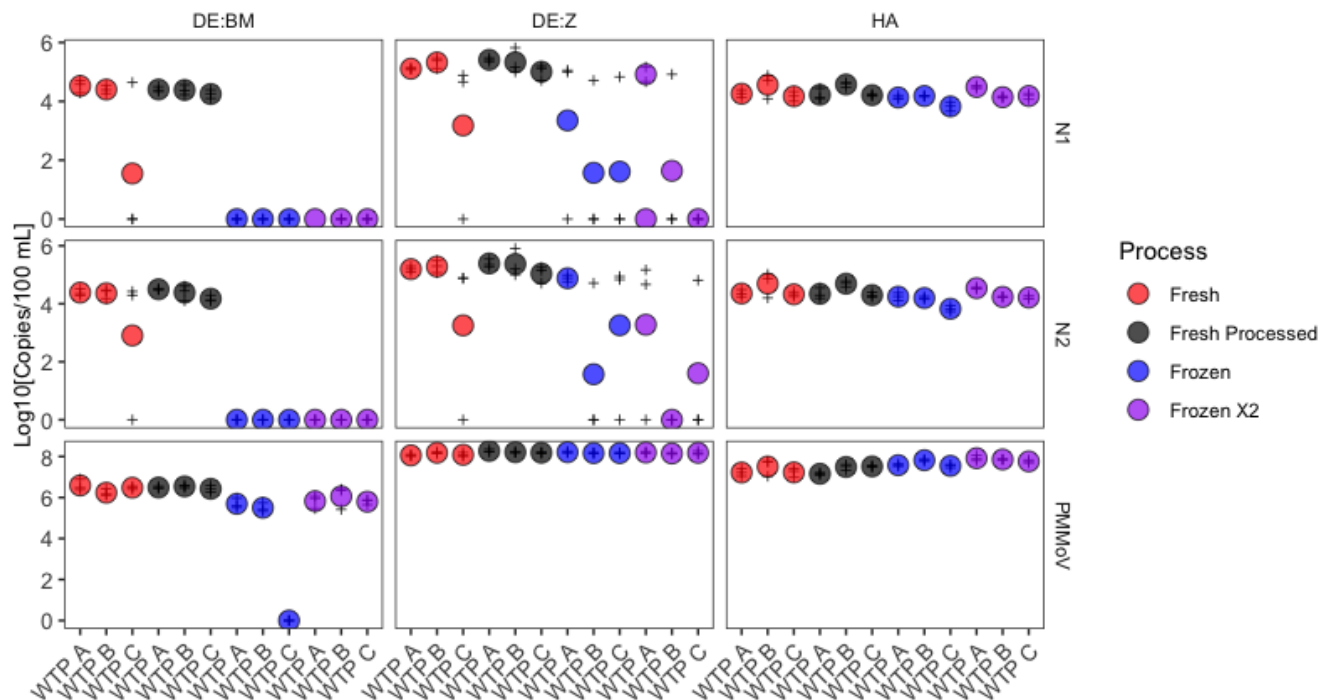
240 Samples which were preserved, then frozen (fresh processed and frozen X2) and then put through a
241 direct extraction resulted in similar concentrations as the samples which did not undergo a second
242 freeze-thaw. Influent held at 4°C, preserved, then frozen (fresh processed) for both the DE:BM and DE:Z
243 direct extraction samples, had concentrations that were nearly the same as those where the preserved
244 sample was stored at 4°C: 4-5 Log₁₀ SARS-CoV-2 N1 and N2 copies per 100ml. Samples which were
245 frozen, thawed, preserved, then frozen again (frozen X2) for influent stored at 4°C and below detection
246 for frozen influent. SARS-CoV-2 N1 and N2 concentrations varied less than 0.5 Log₁₀ with the addition of
247 a freeze-thaw step for influent adsorbed onto a membrane filter.

248

249 All three methods yielded quantifiable PMMoV concentrations when the influent was stored at 4°C and
250 no impact was observed with freezing the preserved or concentrated samples, with the exception of one
251 WTP plant (Fig. 2). Concentrations of PMMV varied less than 0.5 Log₁₀ at 4°C or after a freeze thaw.

252

253

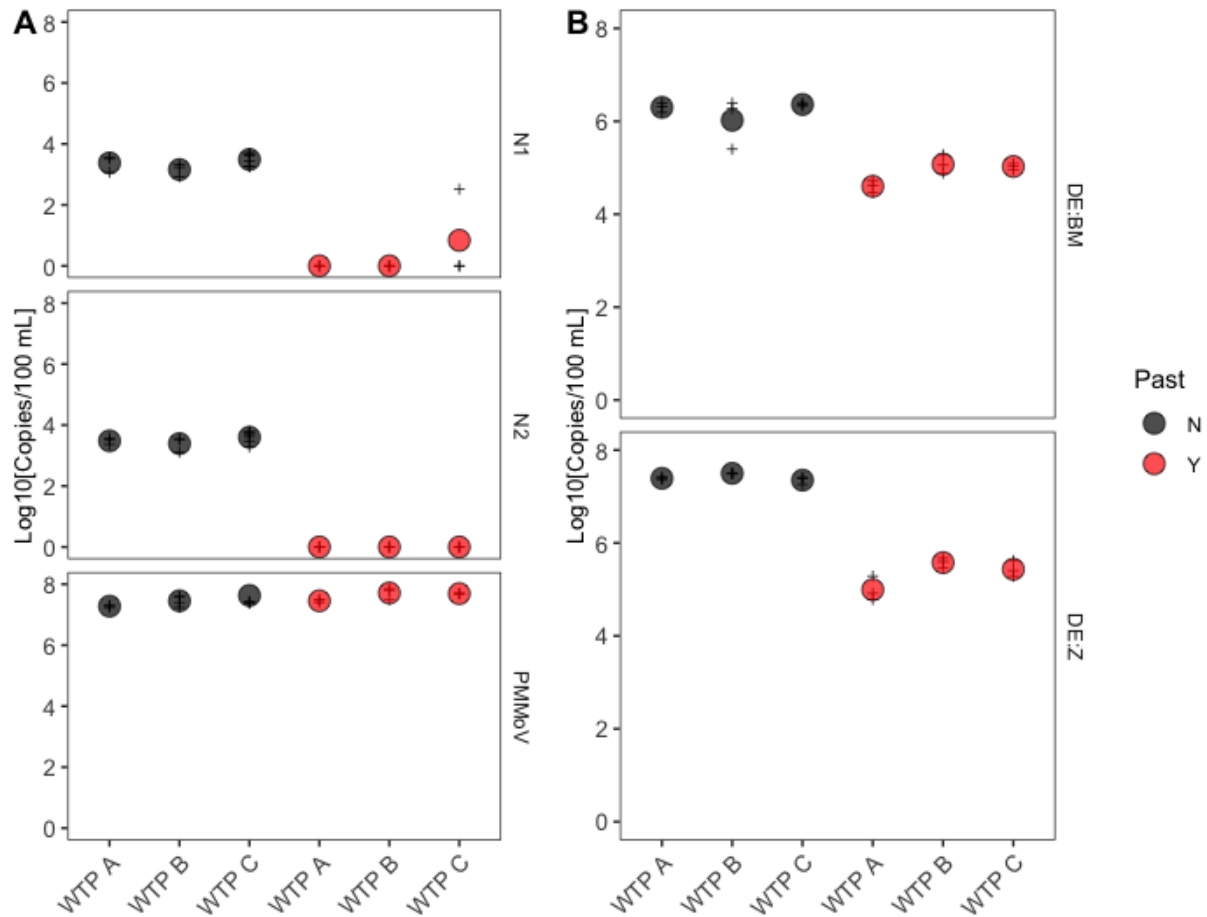


254
 255 **Figure 2.** Comparison of frozen storage methods using samples from 3 WWTP by direct extraction
 256 methods (DE:BM & DE:Z) and membrane adsorption (HA) prior to extraction. Concentrations are
 257 reported in \log_{10} copies per 100ml for N1 (top row), N2 (bottom row), and PMMoV (bottom row). Circles
 258 represent average concentration for the three WTPs and faint crosses represent results from the
 259 individual plants. Fresh represents samples with no freeze-thaw, Fresh Processed represents fresh
 260 influent samples chemically preserved or concentrated on a membrane prior to being frozen, Frozen
 261 represents influent that has gone through one freeze-thaw cycle prior to preservation or concentration,
 262 Frozen X2 is influent that has gone through one freeze thaw, then is preserved or concentrated on a
 263 membrane, then goes through a second freeze thaw prior to extraction.

264
 265
 266 **3.2 Heat Inactivation of Viruses**

267
 268 Heat inactivation at 70°C resulted in a significant reduction, between 1-3 \log_{10} , in SARS-CoV-2 N1
 269 (F=107.1, P<0.001) and N2 (F=3347, P<0.001) concentrations for membrane concentrated samples
 270 (Figure 3A). The SARS-CoV-2 N1 and N2 concentrations were below the limit of detection for all but one
 271 untreated or heat inactivated direct extraction. Therefore, BCoV spike-in recovery concentrations were
 272 compared instead for direct extraction using both the Zymo (DE:Z) and bioMerieux kits (DE:BM) (Figure
 273 3B).

274
 275 Heat inactivation at 70°C resulted in a significant reduction, approximately 2 \log_{10} , in BCoV levels for
 276 samples processed via direct extraction using the Zymo kit (F=132.3, P<0.001). For samples processed by
 277 direct extraction using the bioMerieux, BCoV levels were reduced by approximately 1-2 \log_{10} (F=52.36,
 278 P<0.01, Figure 3). In contrast to SARS-CoV-2 and BCoV, PMMoV concentrations did not significantly
 279 decrease following heat inactivation at 70°C for 40 minutes (F=1.571, P>0.05, Figure 3).



281
 282 **Figure 3.** Concentrations measured with and without pasteurization. Circles represent average
 283 concentration for the three WTPs and faint crosses represent results from the individual plants. Black
 284 circles indicate samples not pasteurized; red circles indicate pasteurized samples; (A) SARS-CoV-2 N1
 285 (top row), SARS-CoV-2 N2 (middle row), and PMMoV (bottom row) levels for samples processed by
 286 membrane adsorption (HA) B) BCoV levels by direct extraction methods (DE:BM & DE:Z).

287
 288

289 3.3 Direct Extraction vs Membrane Adsorption

290

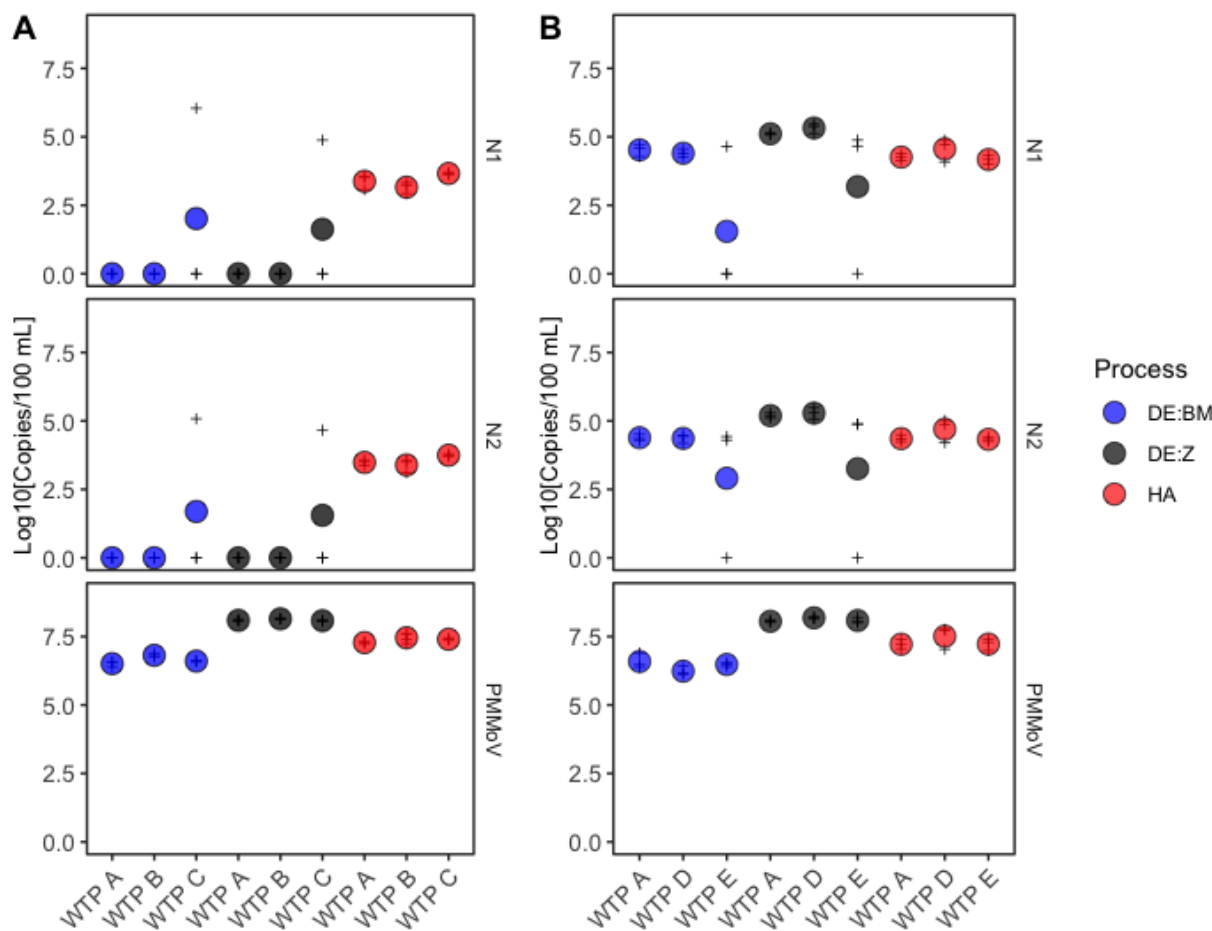
291 Membrane adsorption enabled quantification of viral RNA over a wider range of concentrations
 292 compared to either direct extraction method. Direct extraction using either the bioMerieux (DE:BM) or
 293 Zymo kit (DE:Z) were unable to reliably recover SARS-CoV-2 RNA when the concentrations were low:
 294 10^3 - 10^4 copies per 100ml (Figure 4A). Only the wastewater samples from WTP C had a quantifiable
 295 amount in two of the triplicate samples. The other wastewater samples were all below detection. In
 296 contrast, concentration by membrane adsorption (HA) resulted in measurable, and significantly higher,
 297 concentrations for both N1 (F=10.2, all pairwise P-values <0.05) and N2 (F=15.06, all pairwise P-values
 298 <0.01) when SARS-CoV-2 concentrations were 10^3 - 10^4 copies/100 mL in wastewater.

299

300 At SARS-CoV-2 concentrations of 10^4 - 10^5 copies per 100 mL, direct extraction by both the bioMerieux
 301 (DE:BM) and Zymo kits and membrane adsorption (HA) provided similar concentrations of SARS-CoV-2

302 N1 (F=0.65, all pairwise P-values >0.05) and N2 (F=0.59, all pairwise P-values >0.05) copies and overall
 303 direct extraction was able to more reliably quantify SARS-CoV-2 N1 and N2 copies, than at the lower
 304 concentrations measured (Figure 4B). However, membrane adsorption method (HA) was still the only
 305 method for which all replicates produced quantifiable results.

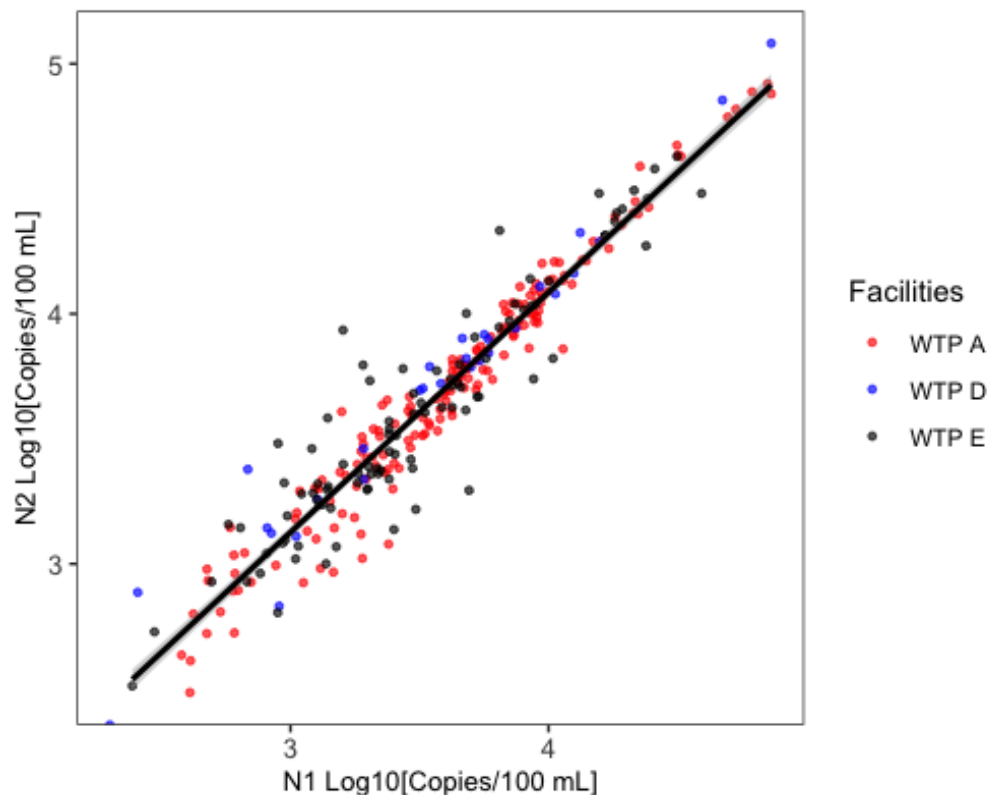
306
 307 All methods were able to produce quantifiable results for PMMOV (Figure 4). Direct extraction using the
 308 Zymo kit (DE:Z) yielded the highest PMMOV copies followed by membrane adsorption (HA), and direct
 309 extraction using the bioMerieux kit (DE:BM).
 310



311
 312
 313 **Figure 4.** Differences between concentration methodology. Color of the circles indicate method used.
 314 HA: membrane adsorption; DE:BM direct extraction with the bioMerieux kit; DE:Z: direct extraction with
 315 the Zymo kit. (A) N1 and N2 levels measured August 2020, during lower levels of SARS-CoV-2 in
 316 wastewater. B) N1 and N2 levels measured December 2020, during higher levels of SARS-CoV-2 in
 317 wastewater. Circles represent average concentration for the three WTPs and faint crosses represent
 318 results from the individual plants.
 319
 320

321 *3.4 Comparison of N1 vs N2 gene targets*
 322

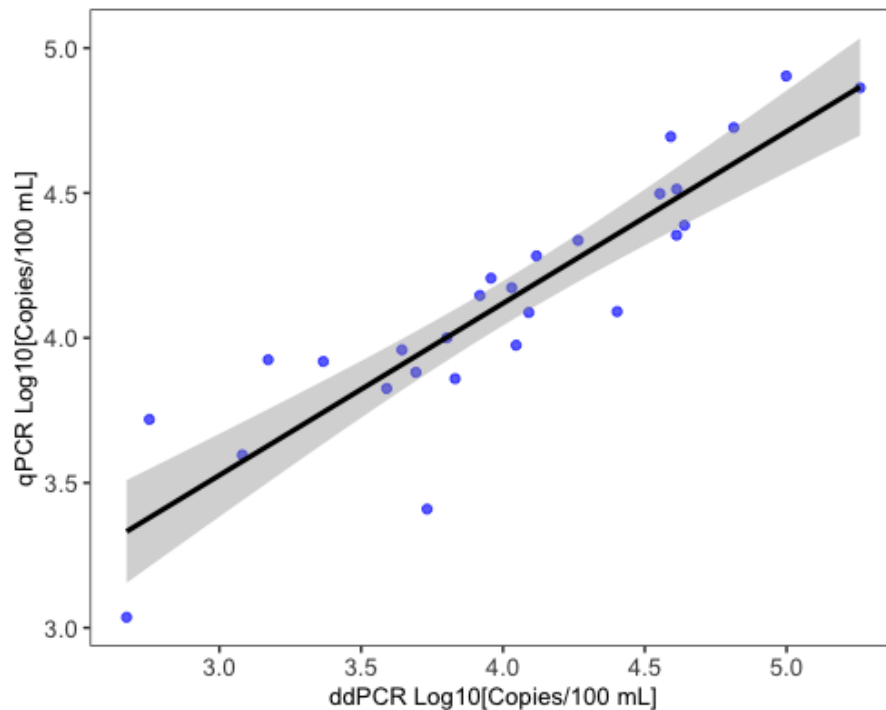
323 The N1 and N2 assays produced similar SARS-CoV-2 concentration measurements in wastewater from 3
324 Southern California treatment plants (Fig 5). The measurements were highly correlated ($R^2=0.95$,
325 $p<0.001$). The slope of the regression line was 1.28, reflecting the generally higher concentrations
326 observed by the N2 assay.
327
328
329



330
331 **Figure 5.** Log10 SARS-CoV-2 in wastewater from three sewage treatment plants measured using the
332 SARS-CoV N1 and N2 assays.
333

334
335 *3.5 Comparison of RT-qPCR to Digital PCR*
336

337 SARS-CoV-2 N1 gene concentrations measured by digital droplet RT-PCR (RT-ddPCR) and RT-qPCR (Fig 6)
338 were highly correlated ($R^2 = 0.80$, $p<0.001$), though there was a slight tendency to higher measurements
339 in RT-qPCR (regression slope of 1.68). The correlation declined in samples with lower SARS-CoV-2
340 concentration. In addition, RT-ddPCR produced detectable, quantifiable concentrations in all 30
341 samples, but RT-qPCR had 3 samples where the gene was not detected and 3 additional samples that
342 were below the limit of quantification.
343
344
345



346
347
348
349
350

Figure 6. Log₁₀ SARS-CoV-2 N1 in wastewater measured using qPCR (y-axis) and digital PCR (x-axis).

351 **4 Discussion**

352
353
354
355
356
357
358
359

Our finding that freezing/thawing of whole influent samples can substantially reduce measured concentrations of SARS-CoV-2 is largely, but not entirely, consistent with other studies that have examined this effect. Wiedhaas et al. (2020) found a 92% reduction in SARS-CoV-2 following freezing influent at ultra-low temperatures for one week prior to processing. Using coronavirus OC43, McMinn et al. (2021) found up to 0.5 log₁₀ reduction after freezing virus solutions for one week at ultra-low temperatures. This result differs from Hokajärvi et al. (2021), who found little reduction from freezing/thawing influent sample using ultra-low freezer temperatures.

360
361
362
363
364
365
366
367

The effect of freezing appears to be easily mitigated in several ways. We found that removing the water matrix and capturing virus on charged filters prior to freezing mitigated this effect. Adding a chemical preservative prior to freezing (e.g., salt, PEG, or an elution solution) has also been reported to reduce viral decay (Whitney et al. 2021, Pecson et al. 2021, McMinn et al. 2021). The observed benefits from adding additional solute particles to the water matrix to mitigate viral decay are consistent with results reported when another solute rich matrix, primary sludge, has been frozen (Graham et al. 2021, Simpson et al. 2021).

368
369
370
371
372
373

Our finding that measurement using qPCR and ddPCR are highly correlated is consistent with other studies in nasopharyngeal swabs (Falzone et al. 2020, Liu et al. 2020), plasma (Tedim et al. 2021), wastewater from aircraft and cruise ships (Ahmed et al. 2020), and raw influent (Cieselski et al. 2021). However, we observed that the correlation became weaker at the lower end of the concentration range we tested, spreading out at lower concentrations in a “broom-shaped” pattern consistent with studies

374 comparing measurements of bacterial targets (Cao et al. 2015). This difference in sensitivity between
375 measurement methods is consistent with ddPCR having up to a 200X lower limit of detection than does
376 qPCR (Cieselski et al. 2021, Ahmed et al. 2021). Furthermore, the digital PCR platform allows for even
377 lower limits of detection by increasing the number of reactions and the number of droplets measured,
378 although at an increase in reaction materials and cost (Huggett et al. 2014). Sensitivity of RT-qPCR could
379 be improved by increasing the volume of RNA extract, but that also increases the amount of inhibitory
380 compounds which come along in wastewater and have been shown to reduce sensitivity when
381 concentrations are low (D'Aoust et al., 2021; Gerrity et al. 2021, Gonzalez et al., 2020; Graham et al.,
382 2021). While not completely immune, digital PCR has been shown to be more robust to inhibition (Cao
383 et al. 2015).

384
385 Our finding that gene target had little effect reinforces several previous reports (e.g. Gerrity et al. 2021,
386 Gonzalez et al 2020, Feng et al. 2021). Even the groups that reported statistically different results among
387 targets (e.g., Pecson et al. 2021) found the difference was less than 10%, much smaller than the other
388 methodological differences we studied. However, our results differ from those of Randazzo et al. (2020)
389 in that we observed that the results from the N1 and N2 gene targets were highly correlated (0.95 vs.
390 0.5). The reason for this difference is likely due to Randazzo measuring low concentration samples using
391 Rt-qPCR; our use of RT-ddPCR helps ameliorate the increasing variability seen in qPCR results as target
392 concentrations near the theoretical limit of quantification.

393
394 Previous studies have been less consistent regarding the effect of heat inactivation (pasteurization). In
395 particular, Pecson et al. (2021) found that pasteurization even caused a slight increase in concentration
396 for some methods (e.g. PEG precipitation), after correction for controls. We found that it caused a 10-
397 1000X decrease, but that may be specific to performing direct extraction with no concentration step.
398 Other authors have found this is of less concern when concentrating samples using PEG precipitation
399 (Pecson et al. 2021) or when NaCl is added prior to performing RNA extraction using silica milk (Whitney
400 et al. 2021). These concentration techniques both use chemicals which will trap viruses, proteins, and
401 nucleic acids (McSharry & Benzinger 1970, Polson 1970, Yamamoto et al. 1970, Lewis and Metcalf 1998)
402 and are using centrifugation to pellet the material which may reduce the loss from virus capsid
403 disruption during pasteurization. In contrast, the membrane adsorption (HA) method uses charge to
404 capture virus particles on an electronegative membrane in the presence of cations and may allow free
405 viral RNA to pass through (Katayama et al. 2002).

406
407 One of our more interesting findings was the tradeoff associated with concentration vs. direct
408 extraction. We found that direct extraction had better recovery compared to concentration on a
409 membrane, but a poorer limit of detection. This is consistent with other studies that have looked at
410 concentration vs direct extraction finding a tradeoff in recovery (Ahmed et al. 2020b, Rusiñol et al. 2020,
411 Pecson et al. 2021). This is likely due to the difference in volume that could be processed by the direct
412 extraction (< 0.5ml) compared to concentration (20ml). While Pecson et al (2021) found some of the
413 highest recoveries from small volume direct extraction, Ahmed et al. (2020) identified HA filtration with
414 cation addition as a good tradeoff of recovery and concentration and Gonzalez et al. (2020) successfully
415 applied this technique to monitor multiple WWTPs. As such, small volume direct extraction without
416 concentration may not be best option with lower SARS-CoV-2 concentrations.

417
418 Our findings appear to have a number of implications for application of WBS. First and foremost, our
419 findings reinforce Pecson et al.'s (2021) suggestion that the same method should be retained when
420 assessing SARS-CoV-2 concentrations over time at a given location. The several orders of magnitude

421 range of different methodological responses we observed were as large as the entire range of values
422 observed at the facilities from which we collected the samples from in this study (Figs 5, 6).

423
424 The second is that methodological differences challenge the ability to make geographic comparisons
425 across facilities that use different methods. Cross-system comparisons are challenging even when using
426 the same methods, as differences in sources among sewersheds (e.g., residential vs. industrial) alters
427 the relationship between RNA and population infectivity, as does transit-time induced differences in
428 decay. A number of studies have attempted to correct for these sewershed difference by normalizing to
429 Pepper Mild Mottle Virus (PMMoV). Unfortunately, our finding that PMMoV is differentially affected by
430 method permutations compared to SARS-CoV-2 makes that correction potentially problematic if
431 different methods are used across facilities, similar to the concerns Kantor et al. (2021) raised about bias
432 in recovery controls. PMMoV concentrations were resilient to pasteurization and to freezing of the raw
433 influent, particularly when compared to the SARS-CoV-2, which is likely due to the biology of the
434 PMMoV as a non-enveloped tobamovirus (Alonso et al. 1991) compared to the enveloped
435 coronaviruses (Zhu et al. 2020). In contrast, the resilience and abundance of PMMoV in sewage is what
436 makes it a good sewage marker and endogenous control (Kitajima et al. 2018). This is consistent with
437 some studies that also reported differentiation in SARS-CoV-2 virus and PMMoV in influent processing
438 (e.g. Whitney et al. 2021), while another study found the two viruses responded consistently to freezing
439 in primary sludge (Simpson et al. 2021).

440
441 Finally, our results indicate that there is considerable difference in sensitivity among methods, which is
442 particularly relevant as we enter a new phase of WBS that focuses on tracking low concentrations of the
443 virus. Until now, the principal advantage of WBS has been speed, providing information a few days
444 sooner than infectivity of individuals. However, the number of clinical testing sites and the inclination of
445 individuals to get tested is declining as vaccination becomes widespread, reducing the reliability of
446 individual infectivity, which has been a primary metric for public health management information. WBS
447 has the potential to become a more reliable indicator of whether there are upticks in prevalence that
448 results as businesses more fully reopen and use of masks and other non-pharmaceutical interventions
449 declines. Addressing this need requires that WBS employ methods sensitive enough to detect low
450 concentrations, rather than producing non-detects.

451
452
453
454
455
456
457
458
459
460
461
462
463
464
465
466
467
468

469 **References**

- 470
- 471 Ahmed, W., Angel, N., Edson, J., Bibby, K., Bivins, A., Brien, J.W.O., Choi, P.M., Kitajima, M., Simpson,
472 S.L., Li, J., Tscharke, B., Verhagen, R., Smith, W.J.M., Zaugg, J., Dierens, L., Hugenholtz, P., Thomas, K. V.,
473 Mueller, J.F., 2020a. First confirmed detection of SARS-CoV-2 in untreated wastewater in Australia: A
474 proof of concept for the wastewater surveillance of COVID-19 in the community. *Sci. Total Environ.* 728,
475 138764.
- 476
- 477 Ahmed, W., Bertsch, P.M., Bibby, K., Haramoto, E., Hewitt, J., Huygens, F., Gyawali, P., Korajkic, A.,
478 Riddell, S., Sherchan, S.P., Simpson, S.L., Sirikanachana, K., Symonds, E.M., Verhagen, R., Vasana, S.S.,
479 Kitajima, M., Bivins, A., 2020b. Decay of SARS-CoV-2 and surrogate murine hepatitis virus RNA in
480 untreated wastewater to inform application in wastewater-based epidemiology. *Environ. Res.* 191,
481 110092.
- 482
- 483 Ahmed, W., Bertsch, P.M., Bivins, A., Bibby, K., Farkas, K., Gathercole, A., Haramoto, E., Gyawali, P.,
484 Korajkic, A., McMinn, B.R., Mueller, J.F., Simpson, S.L., Smith, W.J.M., Symonds, E.M., Thomas, K.V.,
485 Verhagen, R., Kitajima, M., 2020c. Comparison of virus concentration methods for the RT-qPCR based
486 recovery of murine hepatitis virus, a surrogate for SARS-CoV-2 from untreated wastewater. *Sci. Total*
487 *Environ.* 739, 139960.
- 488
- 489 Ahmed, W., Bertsch, P.M., Angel, N., Bibby, K., Bivins, A., Dierens, L., Edson, J., Ehret, J., Gyawali, P.,
490 Hamilton, K.A., Hosegood, I., Hugenholtz, P., Jiang, G., Kitajima, M., Sichani, H.T., Shi, J., Shimko, K.M.,
491 Simpson, S.L., Smith W.J.M., Symonds, E.M., Thomas, K.V., Verhagen, R., Zaugg, J., Mueller, J.F., 2020d.
492 Detection of SARS-CoV-2 RNA in commercial passenger aircraft and cruise ship wastewater: a
493 surveillance tool for assessing the presence of COVID-19 infected travellers. *J. Trav. Med.* 27(5), taaa116.
494
- 495 Ahmed, W.; Simpson, S.; Bertsch, P.; Bibby, K.; Bivins, A.; Blackall, L.; Bofill-Mas, S.; Bosch, A.; Brandao,
496 J.; Choi, P.; Ciesielski, M.; Donner, E.; D'Souza, N.; Farnleitner, A.; Gerrity, D.; Gonzalez, R.; Griffith, J.;
497 Gyawali, P.; Haas, C.; Hamilton, K.; Hapuarachchi, C.; Harwood, V.; Haque, R.; Jackson, G.; Khan, S.; Khan,
498 W.; Kitajima, M.; Korajkic, A.; La Rosa, G.; Layton, B.; Lipp, E.; McLellan, S.; McMinn, B.; Medema, G.;
499 Metcalfe, S.; Meijer, W.; Mueller, J.; Murphy, H.; Naughton, C.; Noble, R.; Payyappat, S.; Petterson, S.;
500 Pitkanen, T.; Rajal, V.; Reyneke, B.; Roman, F.; Rose, J.; Rusinol, M.; Sadowsky, M.; Sala-Comorera, L.;
501 Setoh, Y.X.; Sherchan, S.; Sirikanachana, K.; Smith, W.; Steele, J.; Sabburg, R.; Symonds, E.; Thai, P.;
502 Thomas, K.; Tynan, J.; Toze, S.; Thompson, J.; Whiteley, A.; Wong, J.; Sano, D.; Wuertz, S.; Xagorarakis, I.;
503 Zhang, Q.; Zimmer-Faust, A.; Shanks, O. Minimizing Errors in RT-PCR Detection and Quantification of
504 SARS-CoV-2 RNA for Wastewater Surveillance. *Preprints* **2021**, 2021040481 (doi:
505 10.20944/preprints202104.0481.v1).
- 506
- 507 Alleman, M.M., Rey-Benito, G., Burns, C.C., Vega, E., 2021. Environmental surveillance for poliovirus in
508 Haiti (2017-2019): The dynamic process for the establishment and monitoring of sampling sites. *Viruses.*
509 13(3), 505.
- 510
- 511 Asghar, H., Diop, O.M., Weldegebriel, G., Malik, F., Shetty, S., El Bassioni, L., Akande A.O., Al Maamoun,
512 E., Zaidi, S., Adeniji, A.J., Burns, C.C., Deshpande, J., Oberste, M.S., Lowther, S.A., 2014. Environmental
513 surveillance for polioviruses in the Global Polio Eradication Initiative. *J Infect Dis.* 1(210 Suppl 1), S294-
514 303
- 515

- 516 Bivins, A., North, D., Ahmad, A., Ahmed, W., Alm, E., Been, F., Bhattacharya, P., Bijlsma, L., Boehm, A.B.,
517 Brown, J., Buttiglieri, G., Calabro, V., Carducci, A., Castiglioni, S., Gurol, Z.C., Chakraborty, C., Costa, F.,
518 Curcio, S., de los reyes III, F.L., Delgado Vela, J., Farkas, K., Fernazdez-Casi, X., Gerba, C., Gerrity, D.,
519 Girones, R., Gonzzalez, R., Haramoto, E., Harris, A., Holden, P.A., Ispam, M.T., Jones, D.L., Kasprzyk-
520 Hordern, B., Kitajima, M., Kotlarz, N., Kumar, M., Kuroda, K., La Rosa, G., Malpei, F., Mautus, M.,
521 McLellan, S.L., Medema, G., Meschke, J.S., Mueller, J., Newton, R.J., Noble, R.T., van Nuijs, A., Peccia, J.,
522 Perkins, T.A., Pickering, A.J., Rose, J., Sanchez, G., Smith, A., Stadler, L., Stauber, C., Thomas, K., van der
523 Voorn, T., Wiggington, K., Zhu, K., Bibby, K., 2020. Wastewater-based epidemiology: global collaborative
524 to maximize contributions in the fight against COVID-19. *Environ. Sci. Technol.* 54(13), 7754-7757.
525 Cao, Y., Raith, M.R., Griffith, J.F., 2015. Droplet digital PCR for simultaneous quantification of general and
526 human-associated fecal indicators for water quality assessment. *Water Res.* 70, 337-349.
527
528 Ciesielski, M., Blackwood, D., Clerkin, T., Gonzalez R., Thompson, H., Larson, A., Noble, R., 2021.
529 Assessing Sensitivity and Reproducibility of Two Molecular Workflows for the Detection of SARS-CoV-2
530 in Wastewater (under review).
531
532 D'Aoust, P.M., Mercier, E., Montpetit, D., Jia, J.-J., Alexandrov, I., Neault, N., Baig, A.T., mayne, J., Zhang,
533 X., Alain, T., Langlois, M.-A., Servos, M.R., MacKenzie, M., Figeys, D., MacKenzie, A.E., Garber, T.E.,
534 Delatolla, R., 2020. Quantitative analysis of SARS-CoV-2 RNA from wastewater solids in communities
535 with low COVID-19 incidence and prevalence. *Water Res.* 188, 116560.
536
537 Decaro, N., Elia, G., Campolo, M., Desario, C., Mari, V., Radogna, A., . . . Buonavoglia, C. (2008). Detection
538 of bovine coronavirus using a TaqMan-based real-time RT-PCR assay. *Journal of Virological Methods*,
539 151(2), 167-171. doi:10.1016/j.jviromet.2008.05.016
540
541 Farkas, K., Hillary, L.S., Malham, S.K., McDonald, J.E., Jones, D.L., 2020. Wastewater and public health:
542 the potential of wastewater surveillance for monitoring COVID-19. *Curr Opin Environ Sci Heal* 17, 14–20.
543 <https://doi.org/10.1016/j.coesh.2020.06.001>
544
545 Falzone, L., Musso, N., Gattuso, G., Bongiorno, D., Palermo, C.I., Scalia, G., Libra, M., Stefani, S., 2020.
546 Sensitivity assessment of droplet digital PCR for SARS-CoV-2 detection. *Int. J. Mol. Med.* 46, 957-964.
547
548 Feng, S., Roguet, A., McClary-Gutierrez, J.S., Newton, R.J., Kloczko, N., Meiman, J.G., McLellan, S.L., 2021.
549 Evaluation of sampling frequency and normalization of SARS-CoV-2 wastewater concentrations for
550 capturing COVID-19 burdens in the community. *Medrxiv* 2021.02.17.21251867.
551 <https://doi.org/10.1101/2021.02.17.21251867>
552
553 Gerrity, D., Papp, K., Stoker, M., Sims, A., Frehner, W., 2021. Early-pandemic wastewater surveillance of
554 SARS-CoV-2 in Southern Nevada: Methodology, occurrence, and incidence/prevalence considerations.
555 *Water Res X.* 10, 100086.
556
557 Gonzalez, R., Curtis, K., Bivins, A., Bibby, K., Weir, M.H., Yetka, K., Thompson, H., Keeling, D., Mitchell, J.,
558 Gonzalez., 2020. COVID-19 surveillance in Southeastern Virginia using wastewater-based epidemiology.
559 *Water Res.* 186, 116296.
560
561 Graham KE, Loeb SK, Wolfe MK, Catoe D, Sinnott-Armstrong N, Kim S, Yamahara KM, Sassoubre LM,
562 Mendoza Grijalva LM, Roldan-Hernandez L, Langenfeld K, Wigginton KR, Boehm AB. 2021. SARS-CoV-2

- 563 RNA in wastewater settled solids is associated with COVID-19 cases in a large urban sewershed. *Environ*
564 *Sci. Technol.* 55(1), 488-498.
- 565
- 566 Hart, O. E., & Halden, R. U. 2020. Computational analysis of SARS-CoV-2/COVID-19 surveillance by
567 wastewater-based epidemiology locally and globally: Feasibility, economy, opportunities and challenges.
568 *The Science of the total environment*, 730, 138875. <https://doi.org/10.1016/j.scitotenv.2020.138875>
- 569
- 570 Hokajärvi, A.-M., Rytönen, A., Tiwari, A., Kauppinen, A., Oikarinen, S., Lehto, K.-M., Kankaanpää, A.,
571 Gunnar, T., Al-Hello, H., Blomqvist, S., Miettinen, I.T., Savolainen-Kopra, C., Pitkänen, T., 2020. The
572 detection and stability of the SARS-CoV-2 RNA biomarkers in wastewater influent in Helsinki, Finland.
573 *Sci. Total Environ.* 770, 145274.
- 574
- 575 Hothorn T, Bretz F, Westfall P (2008). "Simultaneous Inference in General Parametric Models."
576 *Biometrical Journal*, 50(3), 346–363.
- 577
- 578 Huggett, J.F., Cowen, S., Foy, C.A., 2015. Considerations for Digital PCR as an Accurate Molecular
579 Diagnostic Tool. *Clin Chem* 61, 79–88. <https://doi.org/10.1373/clinchem.2014.221366>
- 580
- 581 Kantor, R.S., Nelson, K.L., Greenwald, H.D., Kennedy, L.C., 2021. Challenges in Measuring the Recovery of
582 SARS-CoV-2 from Wastewater. *Environ Sci Technol* 55, 3514–3519.
583 <https://doi.org/10.1021/acs.est.0c08210>
- 584
- 585 Katayama, H., Shimasaki, A., Ohgaki, S., 2002. Development of a virus concentration method and its
586 application to detection of enterovirus and Norwalk virus from coastal seawater. *Appl. Environ.*
587 *Microbiol.* 68, 1033–1039.
- 588
- 589 Katayama H, Haramoto E, Oguma K, Yamashita H, Tajima A, Nakajima H, Ohgaki S. One-year monthly
590 quantitative survey of noroviruses, enteroviruses, and adenoviruses in wastewater collected from six
591 plants in Japan. *Water Res.* 2008 Mar;42(6-7):1441-8. doi: 10.1016/j.watres.2007.10.029. Epub 2007 Oct
592 23. PMID: 17996920.
- 593
- 594 Kitajima, M., Sassi, H.P., Torrey, J.R., 2018. Pepper mild mottle virus as a water quality indicator. *Npj*
595 *Clean Water* 1, 19. <https://doi.org/10.1038/s41545-018-0019-5>
- 596
- 597 Kitajima, M., Ahmed, W., Bibby, K., Carducci, A., Gerba, C.P., Hamilton, K.A., Haramoto, E., Rose, J.B.,
598 2020. SARS-CoV-2 in wastewater: State of the knowledge and research needs. *Sci. Total Environ.* 739,
599 139076.
- 600
- 601 La Rosa, G., Iaconelli, M., Mancini, P., Bonanno, G., Ferraro, G.B., Veneri, C., Bonadonna, L., Lucentini, L.,
602 Suffredini, E., 2020. First detection of SARS-CoV-2 in untreated wastewaters in Italy. *Sci. Total Environ.*
603 736, 139652.
- 604
- 605 LaTurner, Z. W., Zong, D. M., Kalvapalle, P., Gamas, K. R., Terwilliger, A., Crosby, T., Ali, P., Avadhanula,
606 V., Santos, H. H., Weesner, K., Hopkins, L., Piedra, P. A., Maresso, A. W., & Stadler, L. B. 2021. Evaluating
607 recovery, cost, and throughput of different concentration methods for SARS-CoV-2 wastewater-based
608 epidemiology. *Water Research*, 197, 117043.
- 609

- 610 Lewis, G. D., & Metcalf, T. G. 1988. Polyethylene glycol precipitation for recovery of pathogenic viruses,
611 including hepatitis A virus and human rotavirus, from oyster, water, and sediment samples. *Applied and*
612 *environmental microbiology*, 54(8), 1983–1988. <https://doi.org/10.1128/aem.54.8.1983-1988.1988>
613
- 614 Lu, X., Wang, L., Sakthivel, S. K., Whitaker, B., Murray, J., Kamili, S....Lindstrom, S. (2020). US CDC Real-
615 Time Reverse Transcription PCR Panel for Detection of Severe Acute Respiratory Syndrome Coronavirus
616 2. *Emerging Infectious Diseases*, 26(8), 1654-1665. <https://doi.org/10.3201/eid2608.201246>.
617
- 618 Liu, C., Shi, Q., Peng, M., Lu, R., Li, H., Cai, Y., Chen, J., Xu, J., Shen, B., 2020. Evaluation of droplet digital
619 PCR for quantification of SARS-CoV-2 virus in discharged COVID-19 patients. *Aging (Albany NY)*. 12 (21),
620 20997-21003.
621
- 622 McCall, C., Wu, H., Miyani, B., & Xagorarakis, I. (2020). Identification of multiple potential viral diseases in
623 a large urban center using wastewater surveillance. *Water research*, 184, 116160.
624 <https://doi.org/10.1016/j.watres.2020.116160>
625
- 626 McMinn, B., Korajkic, A., Kelleher, J., Herrmann, M.P., Pemberton, A.C., Ahmed, W., Villegas, E.N.,
627 Oshima, K., 2021. Development of a Large Volume Concentration Method for Recovery of Coronavirus
628 from Wastewater. *Sci. Total Environ*
629
- 630 McSharry J, Benzinger R. Concentration and purification of vesicular stomatitis virus by polyethylene
631 glycol "precipitation". *Virology*. 1970 Mar;40(3):745–746.
632
- 633 Medema G, Heijnen L, Elsinga G, Italiaander R, Brouwer A: Presence of SARS Coronavirus-2 RNA in
634 Sewage and Correlation with Reported COVID-19 Prevalence in the Early Stage of the Epidemic in the
635 Netherlands. *Environ Sci Technol Lett* 2020, 7:511–516.
636
- 637 Naughton, C.C., Roman Jr., F.A., Alvarado, A.G.F., Tariqi, A.Q., Deeming, M.A., Bibby, K., Bivins, A., Rose,
638 J.B., Medema, G., Ahmed, W., Katsivelis, P., Allan, V., Sinclair, R., Zhang, Y., Kinyua, M.N., 2021. Show us
639 the data: Global COVID-19 wastewater monitoring efforts, equity, and gaps. *MedRXiv*. doi:
640 <https://doi.org/10.1101/2021.03.14.21253564>.
641
- 642 Nemudryi, A., Nemudraia, A., Wiegand, T., Surya, K., Buyukyoruk, M., Cicha, C., Vanderwood, K.K.,
643 Wilkinson, R., Wiedenheft, B., 2020. Temporal detection and phylogenetic assessment of SARS-CoV-2 in
644 municipal wastewater. *Cell Reports Medicine* 1, 100098. <https://doi.org/10.1016/j.xcrm.2020.100098>
645
- 646 Pecson, B.M., Darby, E., Haas, C.N., Amha, Y.M., Bartolo, M., Danielson, R., Dearborn, Y., Giovanni, G.D.,
647 Ferguson, C., Fevig, S., Gaddis, E., Gray, D., Lukasik, G., Mull, B., Olivas, L., Olivieri, A., Qu, Y., 2021.
648 Reproducibility and sensitivity of 36 methods to quantify the SARS-CoV-2 genetic signal in raw
649 wastewater: findings from an interlaboratory methods evaluation in the US. *Environ. Sci.: Water Res.*
650 *Technol*.
651
- 652 Polson, A. 1977 A theory for the displacement of proteins and viruses with polyethylene glycol. *Pre.*
653 *Biochem.* 7, 129-154.
654
- 655 Randazzo, W., Truchado, P., Ferranfo, E.C., Simon, P., Allende, A., Sanchez, G., 2020. SARS-CoV-2 RNA
656 titers in wastewater anticipated COVID-19 occurrence in a low prevalence area. *Water Res.* 115942.
657

658 Rusiñol, M., Martínez-Puchol, S., Forés, E., Itarte, M., Girones, R., Bofill-Mas, S., 2020. Concentration
659 methods for the quantification of coronavirus and other potentially pandemic enveloped virus from
660 wastewater. *Curr. Opin. Environ. Sci. Health*. 17, 21–28.
661
662 Simpson, A., Topol, A., White, B., Wolfe, M. K., Wigginton, K., & Boehm, A. B. (2021). Effect of storage
663 conditions on SARS-CoV-2 RNA quantification in wastewater solids. *medRxiv*.
664
665 Steele, J.A., Blackwood, A.D., Griffith, J.F., Noble, R.T., Schiff, K.C., 2018. Quantification of pathogens and
666 markers of fecal contamination during storm events along popular surfing beaches in San Diego,
667 California. *Water Research* 136, 137–149. <https://doi.org/10.1016/j.watres.2018.01.056>
668
669 Tedim, AP, Almansa, R, Dominguez-Gill, M, Gonzalez-Rivera, M, Micheloud, D, Ryan, P, Mendez, R,
670 Blanca-Lopez, N, Perez-Garcia, F, Bustamante, E, Gomez, JM, Doncel, D, Trapiello, W, Kelvin, AA, Booth,
671 R, Ostadgavahi, AT, Oneizat, R, Puertas, C, Barbe, F, Ferrer, R, Menendez, R, Bermejo-Martin, JF, Eiros,
672 JM, Kelvin, D, Torres, A: Comparison of real-time and droplet digital PCR to detect and quantify SARS-
673 CoV-2 RNA in plasma. *Eur J of Clin Invest*. 2021. 51:e13501. <https://doi.org/eci.13501>
674
675 Torii, S., Furumai, H., Katayama, H., 2020. Applicability of polyethylene glycol precipitation followed by
676 acid guanidinium thiocyanate phenol-chloroform extraction for the detection of SARS-CoV-2 RNA from
677 municipal wastewater. *Sci. Total Environ*. 756, 143067
678
679 Weidhaas, J., Aanderud, Z., Roper, D., VanDerslice, J., Gaddis, E., Ostermiller, J., Hoffman K., Jamal R.,
680 Heck P., Zhang Y., 2020. Correlation of SARS-CoV-2 RNA in wastewater with COVID-19 disease burden in
681 sewersheds.
682
683 Whitney, O.N., Lauren C. Kennedy, Vinson B. Fan, Adrian Hinkle, Rose Kantor, Hannah Greenwald,
684 Alexander Crits-Christoph, Basem Al-Shayeb, Mira Chaplin, Anna C. Maurer, Robert Tjian, and Kara L.
685 Nelson. 2021 Sewage, Salt, Silica, and SARS-CoV-2 (4S): An Economical Kit-Free Method for Direct
686 Capture of SARS-CoV-2 RNA from Wastewater. *Environmental Science & Technology* 55 (8), 4880-
687 4888 DOI: 10.1021/acs.est.0c08129
688
689 Yamamoto, K.R., Alberts, B.M., Benzinger, R., Lowhorne, L. and Trieber, G. (1970) Rapid bacte-
690 riphage sedimentation in the presence of polyethylene glycol and its application to large scale virus purification.
691 *Virology* 40, 734-744.
692
693
694
695
696
697
698
699
700
701
702
703
704